Proton scattering from the unstable neutron-rich nucleus ^{43}Ar

F. Maréchal,[1,*] T. Suomijärvi,[1] Y. Blumenfeld,[1] A. Azhari,[2,3,†] D. Bazin,[2] J. A. Brown,[2,‡] P. D. Cottle,[4] M. Fauerbach,[2,3,*]
T. Glasmacher,[2,3] S. E. Hirzebruch,[1] J. K. Jewell,[4,§] J. H. Kelley,[1,∥] K. W. Kemper,[4] P. F. Mantica,[2,5] D. J. Morrissey,[2,5]
L. A. Riley,[4,¶] J. A. Scarpaci,[1] H. Scheit,[2,3,**] and M. Steiner[2]

[1]*Institut de Physique Nucléaire, IN$_2$P$_3$-CNRS, 91406 Orsay, France*
[2]*National Superconducting Cyclotron Laboratory, Michigan State University, East Lansing, Michigan 48824*
[3]*Department of Physics and Astronomy, Michigan State University, East Lansing, Michigan 48824*
[4]*Department of Physics, Florida State University, Tallahassee, Florida 32306*
[5]*Department of Chemistry, Michigan State University, East Lansing, Michigan 48824*
(Received 2 June 1999; published 22 November 1999)

The neutron-rich argon isotope ^{43}Ar has been studied by quasielastic and inelastic proton scattering performed in inverse kinematics. The measured inelastic angular distribution for the second excited state is in good agreement with an $L=2$ transition. Assuming this transition to be $E2$, yields a β_2 value for this state of 0.25 ± 0.03 when compared with distorted-wave Born approximation calculations. This value is comparable to the one reported for the stable isotope ^{40}Ar. Moreover it is similar to those measured by Coulomb excitation for the neighboring even-even isotopes ^{42}Ar and ^{44}Ar indicating that the structure of the argon isotopes is stable as a function of neutron number. [S0556-2813(99)03012-5]

I. INTRODUCTION

The availability of radioactive beams with sizeable intensities and good optical qualities makes possible the study of direct reactions induced by unstable nuclei. The study of nuclear matter distributions, deformation, and the modification of shell structure far from stability can be addressed through inverse kinematics reactions on light targets. Considerable interest is currently being focused on neutron-rich nuclei near the $N=28$ magic number for which shell closure is expected to vanish, yielding a new region of deformation [1,2]. The $0^+_{gs} \rightarrow 2^+_1$ transition in even-even neutron rich sulfur and argon isotopes was recently studied by intermediate energy Coulomb excitation [3,4]. The measurement of the excitation energies and the $B(E2)$ reduced transition probabilities showed a weakening of the $N=28$ shell closure that was more pronounced for ^{44}S than for ^{46}Ar. Additional information on the structure of nuclei in this mass region can be obtained from proton scattering experiments. Elastic scattering will give insight into nuclear densities and interaction potentials, while the comparison of Coulomb excitation with proton inelastic scattering should allow neutron and proton deformations to be separated.

We have undertaken a study of the neutron-rich sulfur isotopes through elastic and inelastic scattering of protons in inverse kinematics. We performed experiments on ^{38}S and ^{40}S by using secondary fragmentation beams of ^{38,40}S delivered by the National Superconducting Cyclotron Laboratory at Michigan State University [5,6]. During the second experiment, data were also collected for the neutron-rich isotope ^{43}Ar which was present as a byproduct in the secondary beam. Few of the properties of ^{43}Ar are known, even though several excited states were identified in a previous exotic transfer reaction study [7]. For instance, no spin assignments exist for either the ground or excited states. Here, we present the results of quasielastic and inelastic proton scattering on the unstable nucleus ^{43}Ar performed in inverse kinematics. The low-lying level structure of ^{43}Ar is discussed. The inelastic scattering data are shown to be best described by an $L=2$ transition when compared with distorted-wave Born approximation (DWBA) calculations. The β_2 value extracted from these data, assuming an $E2$ inelastic transition, is compared to the values obtained for the nearby argon isotopes.

II. EXPERIMENT

The secondary ^{43}Ar beam was produced by fragmentation of a primary ^{48}Ca beam at 60 MeV/nucleon, provided by the K1200 cyclotron at the National Superconducting Cyclotron Laboratory, on a 285 mg/cm^2 Be production target. The fragments were analyzed using the A1200 fragment separator [8] and the resulting beam was purified by using a 70 mg/cm^2 aluminum wedge. While the beam optics and A1200 parameters were both optimized for the production of ^{40}S at 30 MeV/nucleon, a final intensity of about 16 000 particles per second (pps) for ^{43}Ar at 33 MeV/nucleon was obtained. The ^{40}S intensity was only 2000 pps. The incident beam nuclei were identified event by event by the combination of a
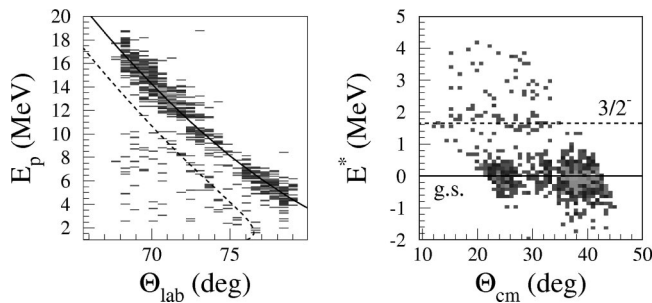
FIG. 1. Energy vs laboratory angle scatterplot (left panel) and excitation energy vs center-of-mass angle scatterplot (right panel) for recoiling protons in coincidence with the ^{43}Ar ejectiles. Solid and dashed lines are the calculated energy-angle correlations for the elastic scattering and the inelastic scattering to the second excited state located at 1.61 MeV.

time-of-flight measurement over a 36 meter long flight path and a total energy measurement using a phoswich detector placed behind the secondary hydrocarbon scattering target.

The experimental setup is described in detail in Ref. [6] and only the most important features will be repeated here. The ^{43}Ar beam was scattered by a thin 2 mg/cm^2 (CH$_2$)$_n$ target which allowed accurate angle definition to be obtained, even for low-energy protons. A group of eight telescopes, 5×5 cm^2 active area each, was used to measure the energies and angles of the recoiling protons. Each telescope was composed of a 300 μm thick silicon strip detector with 16 vertical strips (3 mm wide) followed by a second 500 μm thick silicon detector and a 1 cm thick stopping cesium-iodide detector read out by four photodiodes. The silicon-strip array was positioned 29 cm from the scattering target and covered the laboratory angles between 56° and 89°, allowing us to measure elastic and inelastic angular distributions over the center-of-mass angular range $\Theta_{cm} = 15°$ to $\Theta_{cm} = 45°$. This setup has a dynamic range for protons from about 1 up to 50 MeV. The particle identification in the telescopes was performed either by a time-of-flight measurement for low-energy particles stopped in the silicon strip detector, or by a ΔE-E measurement for higher energy particles that punched through the first detector.

The data in the silicon strip telescopes were taken in coincidence with a zero degree ΔE-E plastic detector which identified the outgoing fragments and allowed the elastic and inelastic reaction channels to be selected, thus very effectively reducing the background in the proton detectors. This plastic detector also yielded a start signal for the proton time-of-flight measurements. Due to the poor emittance of the secondary ^{43}Ar beam ($\sim 100\pi$ mm mrad), two parallel plate avalanche counters, placed 82 cm and 183 cm upstream from the target, were used to measure event by event the incident beam angle and beam position on the target. This beam tracking allowed us to improve the reconstruction of the reaction kinematics.

The left panel of Fig. 1 displays the data obtained for recoiling protons, in coincidence with the ^{43}Ar ejectiles, in an energy vs laboratory angle scatterplot. The data were then transformed to the center-of-mass frame using relativistic kinematics and the correlations between the excitation energy
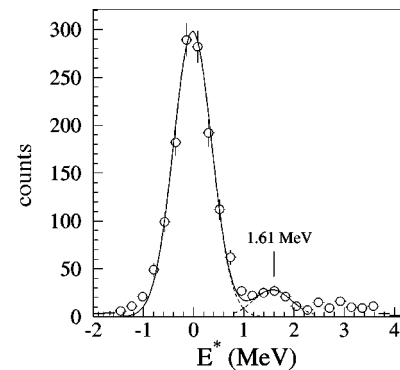

FIG. 2. Excitation energy spectrum measured for ^{43}Ar. The dashed lines are Gaussian fits to the quasielastic and second excited state peaks. The solid line is the sum of the two contributions.

E^* and the center-of-mass angle Θ_{cm} are shown on the right panel of Fig. 1. The scattering angle has been corrected for the incident beam angle as well as for its impact position on the target. Despite the low statistics, the elastic scattering (solid line) and inelastic scattering to the second excited state (dashed line) are clearly separated in both spectra.

Figure 2 shows the excitation energy spectrum for ^{43}Ar where, in addition to the elastic peak, a peak centered at 1.61 ± 0.04 MeV is observed. The excitation energy resolution is of the order of 850 keV which is very similar to that measured for a stable ^{40}Ar beam with the same detection system [5]. Significant cross section above 2.2 MeV is also observed but the low statistics and the energy resolution do not allow us to resolve these peaks.

Figure 3 shows the angular distributions for the elastic peak and the excited-state peak of ^{43}Ar located at 1.61 MeV. These distributions were obtained by projecting the contents of two different excitation energy cuts in the excitation energy vs Θ_{cm} plane. The absolute normalization of the data was obtained using the incident beam intensity given by the 0° detector and the target thickness. The error bars on the cross section are purely statistical and the error in Θ_{cm} is equal to the bin size and is shown on the figure.
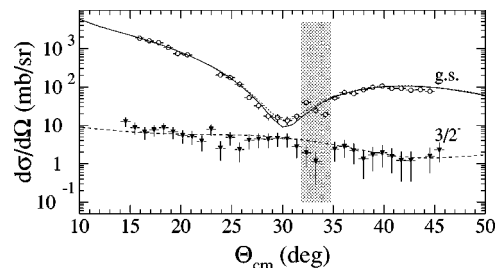

FIG. 3. Angular distributions for the quasielastic scattering and inelastic scattering to the second excited state measured for the ^{43}Ar(p,p') reaction at 33 MeV/nucleon. The solid and the dashed lines are DWBA calculations with the Becchetti-Greenlees optical potential [14]. The dotted line is the calculated quasielastic angular distribution assuming a β_2 value of 0.25 for the $\frac{7}{2}^-$ first excited state. The vertical dotted region corresponds to the crossing between the 500 μm silicon detector and the CsI detector.

III. ANALYSIS

Little is known about the structure of ^{43}Ar. Some insight regarding the low-lying structure of ^{43}Ar can be obtained from an examination of neighboring nuclei. The ground state of the closed proton shell $N=25$ isotone ^{45}Ca has $J^\pi = 7/2^-$ (the lowest lying $\nu f_{7/2}^{-3}$ state), but a $\nu f_{7/2}^{-3}$ $J^\pi = 5/2^-$ state lies at an excitation energy of only 174 keV [9]. The isotope ^{41}Ar bears some similarity to ^{43}Ar because it has three $f_{7/2}$ neutron *particles* instead of the three $f_{7/2}$ neutron *holes* in ^{43}Ar (of course, both nuclei have two sd proton holes—predominantly $d_{3/2}$—in their lowest lying states). Once again, J^π for the ground state is $7/2^-$ [deduced by Endt [9] on the basis of data from a ^{40}Ar$(d,p)^{41}$Ar measurement] with a $J^\pi = 5/2^-$ state at 178 keV. Endt [9] cited a β-decay result which limited the ground-state spin of ^{43}Ar to either 3/2 or 5/2; however, no independent report of this result was ever published. In a shell-model analysis of ^{43}Ar, Warburton [10] predicts that the $J^\pi = 5/2^-$ and $J^\pi = 7/2^-$ states reverse their order but remain close in energy, with a $J^\pi = 5/2^-$ ground state and a $J^\pi = 7/2^-$ state at an excitation energy of 22 keV. It would not be reasonable to assume a unique spin assignment for the ground state based on this result; however, it seems quite likely that the ground state of ^{43}Ar is dominated by the $\pi d_{3/2}^{-2} \nu f_{7/2}^{-3}$ configuration and has $J^\pi = 5/2^-$ or $7/2^-$.

In the neighboring even-even nuclei ^{42,44}Ar, the 2_1^+ states (which occur at 1.21 and 1.14 MeV, respectively [11,3]) are connected to the ground states with collective $E2$ transitions corresponding to $\beta_2 \approx 0.25$. Therefore, we would expect a low-lying concentration of $E2$ strength—resulting from the coupling of a collective quadrupole excitation to the ground state—in ^{43}Ar as well. The 1.61 MeV peak observed in the present (p,p') reaction is quite likely to correspond to this expected concentration of $E2$ strength. The systematic study of octupole states in this mass region in Ref. [12] implies that strong octupole states do not occur below 3.5 MeV in neutron-rich Ar isotopes.

For the present analysis of our data on ^{43}Ar, we will assume that the ground state of ^{43}Ar has $J^\pi = 5/2^-$, and that a first excited state of $J^\pi = 7/2^-$ occurs at 200 keV (and cannot be separated from the ground state in the present experiment). Explicit inclusion of the $J^\pi = 7/2^-$ excited state may be important because it is likely that a strong $E2$ matrix element connects the two members of the ground-state doublet in ^{43}Ar as is the case in ^{41}Ar [9]. Since the members of the ground-state doublet cannot be experimentally separated, we must regard the ''ground-state angular distribution'' as a quasielastic scattering angular distribution.

Distorted-wave Born approximation calculations were performed using the code ECIS [13] and the results are compared to the data in Fig. 3. The optical potential parameters were taken from the Becchetti-Greenlees parametrization [14], which was developed for elastic proton scattering on $A \geqslant 40$ nuclei. A good reproduction of the elastic-scattering data for the even-even sulfur isotopes between $A=32$ and $A=40$ was previously obtained with the same optical model parametrization [6]. The solid line in Fig. 3 shows the results of a calculation of elastic scattering only—that is, excitation
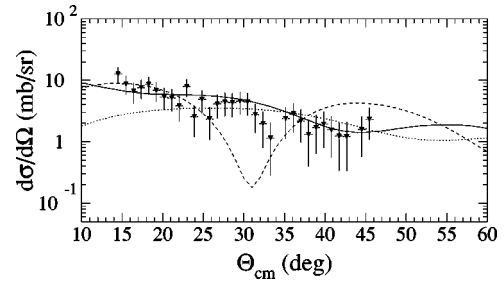

FIG. 4. DWBA cross-section calculations, using the Becchetti-Greenlees optical potential [14], for the transition to the second excited state in ^{43}Ar. The solid line is for an $L=2$ transition. The dashed and dotted lines are for $L=1$ and $L=3$, respectively.

of the possible $7/2^-$ member of the ground-state doublet was neglected. The calculation reproduces the data quite well. A second calculation was performed in which the differential cross section for inelastic scattering to an assumed $7/2^-$ state at 200 keV is *added* to the elastic scattering differential cross section, assuming a coupling constant $\beta_2 = 0.25$. This value was chosen because it is approximately equal to the β_2 values found in the neighboring Ar isotopes for low-lying quadrupole excitations. The result of this ''quasielastic scattering'' calculation is shown as the dotted line in Fig. 3. It is clear from the figure that the inelastic contribution to the quasielastic peak is quite small and has little effect on how well the data are reproduced.

Figure 4 displays the results of DWBA cross-section calculations for the inelastic scattering to the second excited state in ^{43}Ar, assuming different possible L transitions in order to determine the L transfer for the observed inelastic-scattering data. The solid line corresponds to a calculation which assumes an $L=2$ transition between the ground state and the second excited state. The dashed and dotted lines correspond to calculations assuming $L=1$ and $L=3$ transitions, respectively. The comparison of the calculations with the experimental data clearly shows that the inelastic-scattering process does not proceed through an $L=1$ transition. Ruling out a possible $L=3$ transition is not so simple since the calculated angular distribution is relatively flat for this case. However, no normalization of the calculation to the data could describe simultaneously the data at 10° and 40°. The best overall normalization to the data is shown in Fig. 4, where the forward angles are underestimated by a factor of 3. Therefore, the $L=3$ transition is also found to be not suitable. The best overall description of the experimental inelastic angular distribution is obtained when an $L=2$ transition is assumed between the ground state and the second excited state of ^{43}Ar. This last calculation was performed using a standard vibrational form factor and a coupling constant $\beta_2 = 0.25$ to which we assign an experimental uncertainty $\Delta\beta_2 = 0.03$. This calculation is also shown by the dashed line in Fig. 3, along with the calculated elastic angular distribution.

Since the parities of the states are not known, conservation rules allow both electric and magnetic transitions to occur. But, in the low-energy range, the spin-independent isovector central part of the interaction potential is the stron-

gest, favoring mass excitations such as electric quadrupole excitations [15]. At higher proton energies (150–200 MeV), the spin-dependent coupling has its maximum strength relative to the mass coupling, making the unnatural parity transitions, or spin excitations, to be seen with the greatest clarity in this energy region. However, in the energy region of the present experiment, the $M2$ excitation is insignificant and only the $E2$ excitation must be considered. This statement implies that the ground state and the second excited state must have the same parity. As previously mentioned, it is very likely that the ground state of ^{43}Ar is dominated by the $\pi d_{3/2}^{-2} \nu f_{7/2}^{-3}$ configuration, and therefore has a negative parity, though no definite spin can be assigned to that state. This means that the second excited state has also a negative parity and must be dominated by a configuration where the valence neutrons occupy the fp shell. Unusual configurations, for instance $\nu d_{3/2}^{-1} f_{7/2}^{-2}$ particle-hole excitations, seem to be less likely. This result is consistent with an assignment of $J^\pi = 3/2^-$ for the second excited state which one would make based on the known spin value in ^{44}Ca.

The $E2$ deformation parameter extracted here is approximately equal to those determined for ^{42}Ar and ^{44}Ar via electromagnetic probes [$\beta_2 = 0.27(2)$ for ^{42}Ar [11] and $\beta_2 = 0.24(2)$ for ^{42}Ar [3]]. Of course, low-energy proton scattering and electromagnetic probes measure different quantities. Electromagnetic probes measure the proton multipole matrix element while low-energy proton scattering is much more sensitive to the neutron matrix element [16]. However, it is not expected that large differences would occur between proton and neutron deformation parameters in open-shell nuclei like the midneutron shell argon isotopes being discussed here.

IV. CONCLUSIONS

In summary, we have measured angular distributions for quasielastic and inelastic scattering of protons on the unstable nucleus ^{43}Ar. The measured inelastic angular distribution for the second excited state, located at 1.61 ± 0.04 MeV, is in good agreement with an $L=2$ transition. Assuming $E2$ for this transition yields $\beta_2 = 0.25 \pm 0.03$ when compared with DWBA calculations. This deformation is comparable in magnitude with those measured for the neighboring argon nuclei. Though no absolute spin assignment was possible, it is very likely that both the ground state and the second excited state of ^{43}Ar have negative parity. Systematics in this region would suggest $J^\pi = 3/2^-$ for this second excited state. The β_2 value extracted for ^{43}Ar suggests that the structure of the argon isotopes evolves smoothly when the number of neutrons is increased.

[1] A. Poves, and J. Retamosa, Nucl. Phys. **A571**, 221 (1994).

[2] T.R. Werner, J.A. Sheikh, M. Misu, W. Nazarewicz, J. Rikovska, K. Heeger, A.S. Umar, and M.R. Strayer, Nucl. Phys. **A597**, 327 (1996).

[3] H. Scheit, T. Glasmacher, B.A. Brown, J.A. Brown, P.D. Cottle, P.G. Hansen, R. Harkewicz, M. Hellstrom, R.W. Ibbotson, J.K. Jewell, K.W. Kemper, D.J. Morrissey, M. Steiner, P. Thirolf, and M. Thoennessen, Phys. Rev. Lett. **77**, 3967 (1996).

[4] T. Glasmacher, B.A. Brown, M.J. Chromik, P.D. Cottle, M. Fauerbach, R.W. Ibbotson, K.W. Kemper, D.J. Morrissey, H. Scheit, D.W. Sklenicka, and M. Steiner, Phys. Lett. B **395**, 163 (1997).

[5] J.H. Kelley, T. Suomijärvi, S.E. Hirzebruch, A. Azhari, D. Bazin, Y. Blumenfeld, J.A. Brown, P.D. Cottle, S. Danczyk, M. Fauerbach, T. Glasmacher, J.K Jewell, K.W. Kemper, F. Maréchal, D.J. Morrissey, S. Ottini, J.A. Scarpaci, and P. Thirolf, Phys. Rev. C **56**, R1206 (1997).

[6] F. Maréchal, T. Suomijärvi, Y. Blumenfeld, A. Azhari, E. Bauge, D. Bazin, J.A. Brown, P.D. Cottle, J.P. Delaroche, M. Fauerbach, M. Girod, T. Glasmacher, S.E. Hirzebruch, J.K. Jewell, J.H. Kelley, K.W. Kemper, P.F. Mantica, D.J. Morrissey, L.A. Riley, J.A. Scarpaci, H. Scheit, and M. Steiner, Phys. Rev. C **60**, 034615 (1999).

[7] N.A. Jelley, K.H. Wilcox, R.B. Weisenmiller, G.J. Wozniak, and J. Cerny, Phys. Rev. C **9**, 2067 (1974).

[8] B.M. Sherrill, D.J. Morrissey, J.A. Nolen, Jr., N. Orr, and J.A. Winger, Nucl. Instrum. Methods Phys. Res. B **70**, 298 (1992).

[9] P.M. Endt, Nucl. Phys. **A521**, 1 (1990).

[10] E.K. Warburton, Phys. Rev. C **44**, 268 (1991).

[11] S. Raman, C.H. Malarkey, W.T. Milner, C.W. Nestor, Jr., and P.H. Stelson, At. Data Nucl. Data Tables **36**, 1 (1987).

[12] P.D. Cottle and K.W. Kemper, Phys. Rev. C **41**, 259 (1990).

[13] J. Raynal, Phys. Rev. C **23**, 2571 (1981); J. Raynal, CEA Report No. CEA-N-2772, 1994.

[14] F.D. Becchetti, Jr. and G.W. Greenlees, Phys. Rev. **182**, 1190 (1969).

[15] F. Petrovich, J.A. Carr, and H. McManus, Annu. Rev. Nucl. Part. Sci. **36**, 29 (1986).

[16] A.M. Bernstein, V.R. Brown, and V.A. Madsen, Phys. Lett. B **103**, 255 (1981).